Electronic Supplementary Material (ESI) for Journal of Materials Chemistry A.

Lithiation across Interconnected V_2O_5 Nanoparticle Networks

Luis R. De Jesus[a]†, Ying Zhao[b]†, Gregory A. Horrocks[a], Justin L. Andrews[a], Peter Stein[b], Bai-Xiang Xu[b],* and Sarbajit Banerjee[a]*

[a]Department of Chemistry and Department of Materials Science and Engineering, Texas A&M University, College Station, TX 77845-3012; E-mail: banerjee@chem.tamu.edu

[b]Insititute of Materials Science, Mechanik funktionaler Materialien, Technische Universität Darmstadt, Jovanka-Bontschits-Str. 2, 64287 Darmstadt, Germany. E-mail: xu@mfm.tu-darmstadt.de

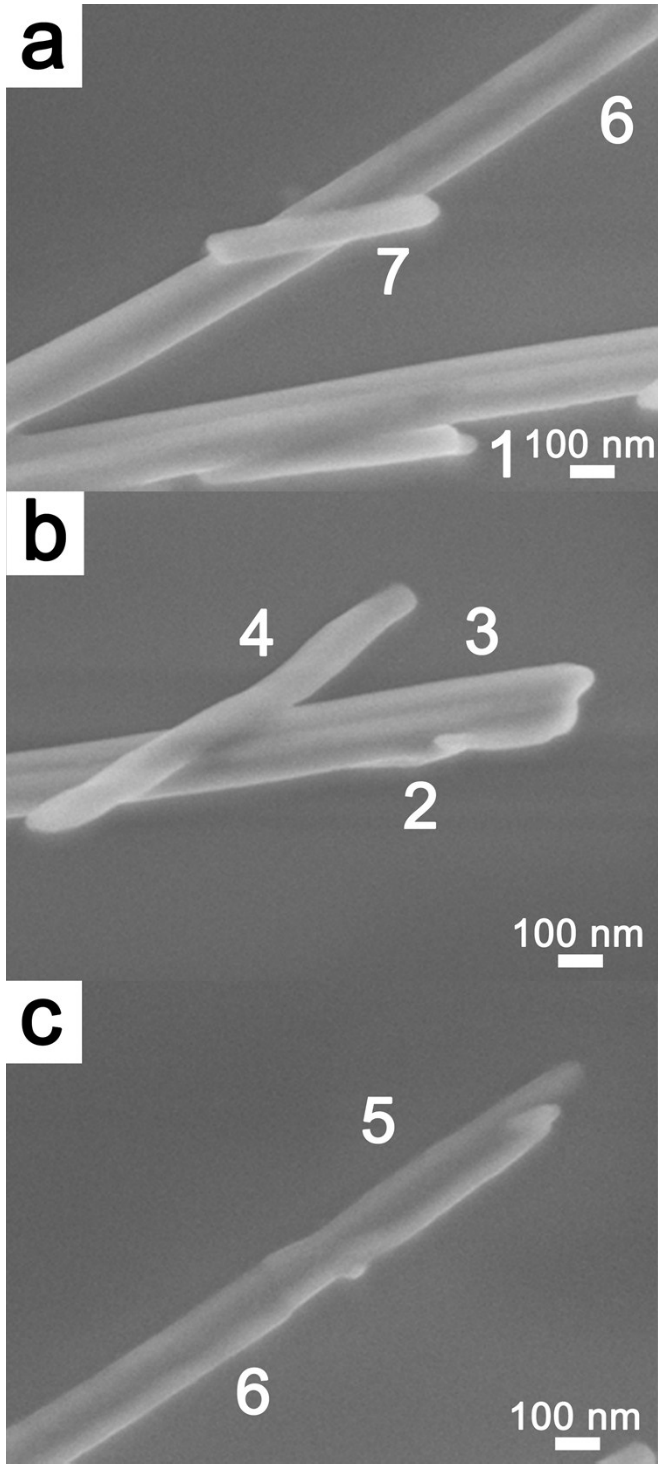

Figure S1. Magnified high-resolution SEM images of a cluster of lithiated particles. High-resolution SEM images providing a magnified view of the particle cluster shown in Figure 1a. (a) Regions **1**, **2**, **3**, **6**, and **7**; (b) region **4** sits atop regions **2** and **3** (intimate contact with **3**); and (c) an imperfection (screw dislocation or surface step) separates one nanowire into regions **5** and **6**.

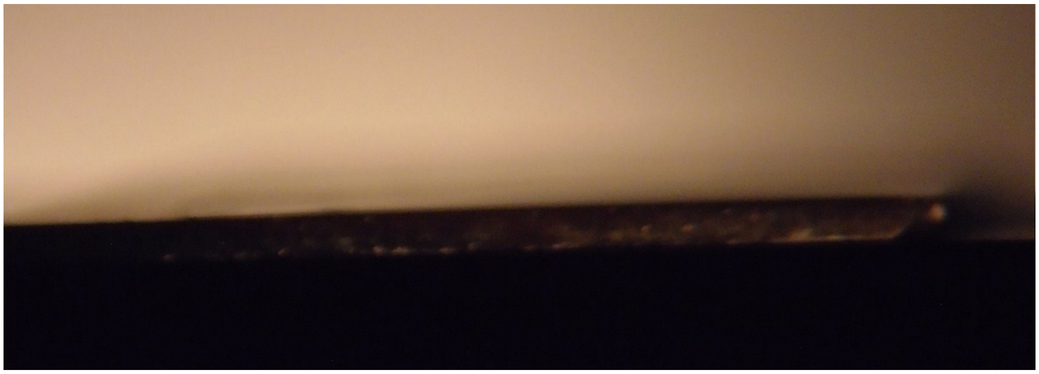

Figure S2. Contact angle measurement of pristine V_2O_5 with a droplet of hexanes. Contact angle measurements for hexanes on a layer of V_2O_5 nanowires suggests immediate and complete spreading of the liquid droplet to a contact angle of 0°.

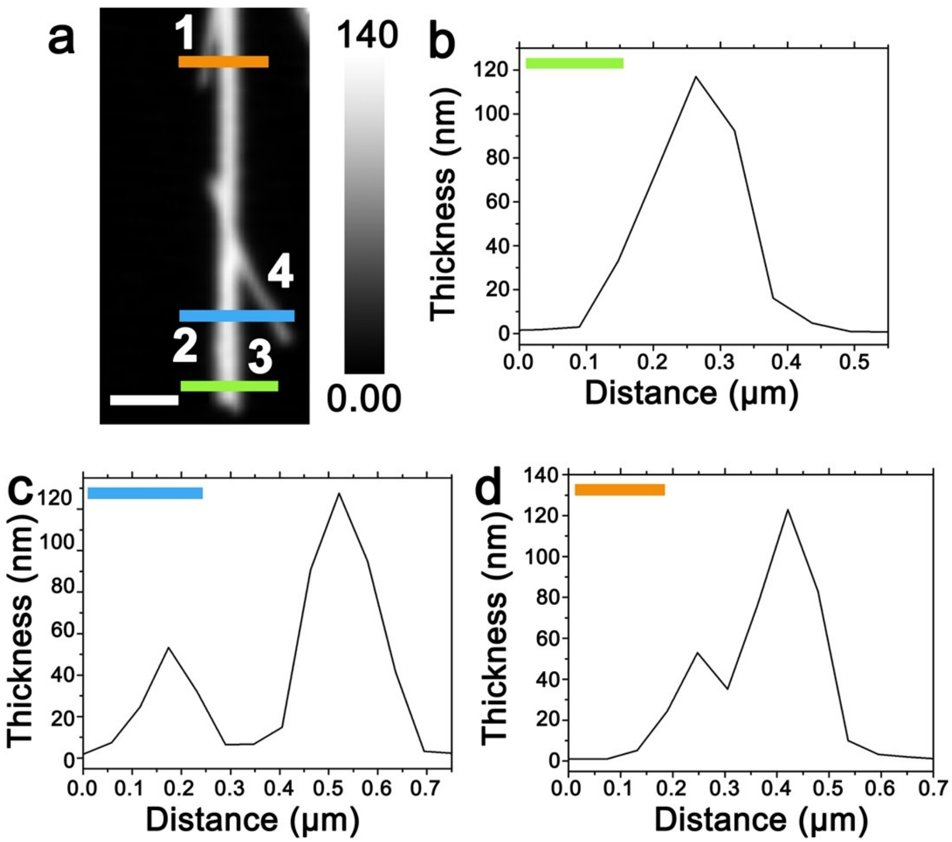

Figure S3. Mapping of optical density in regions 1-4. Thickness map (a) for regions **1**-**4** correlated directly to Figure 2; the gray scale represents the thickness in nanometers. Several line profiles acquired across the optical density image are plotted and allow for elucidation of nanowire thicknesses of (b) regions **2**-**3**; (c) regions **2**-**4**, and (d) regions **1**-**3**.

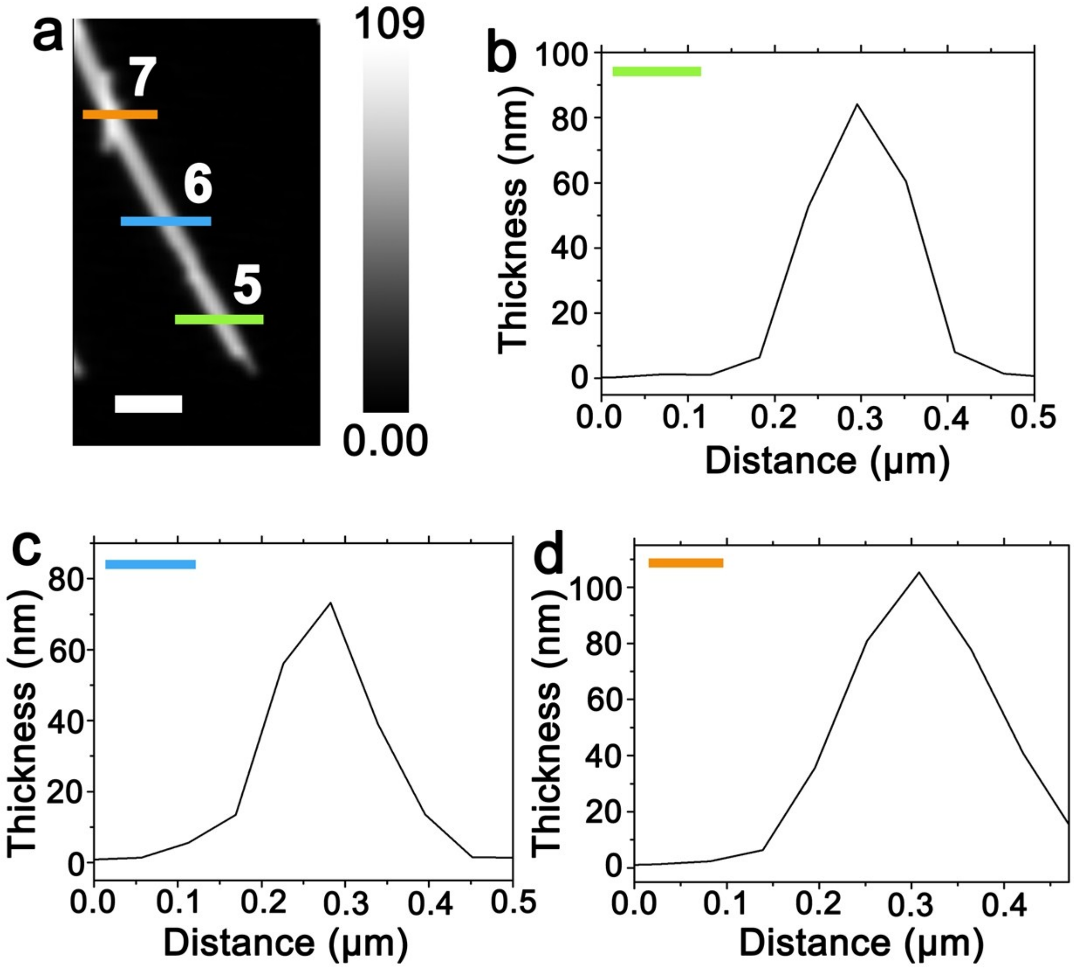

Figure S4. Mapping of optical density in regions 5-7.
Thickness map (a) for regions **5**—**7** correlated directly to figure 3; the gray scale represents the thickness in nm. Several line profiles acquired across the optical density image are plotted and allow for elucidation of nanowire thicknesses of (b) region **5**; (c) region **6**, and (d) region **7**.

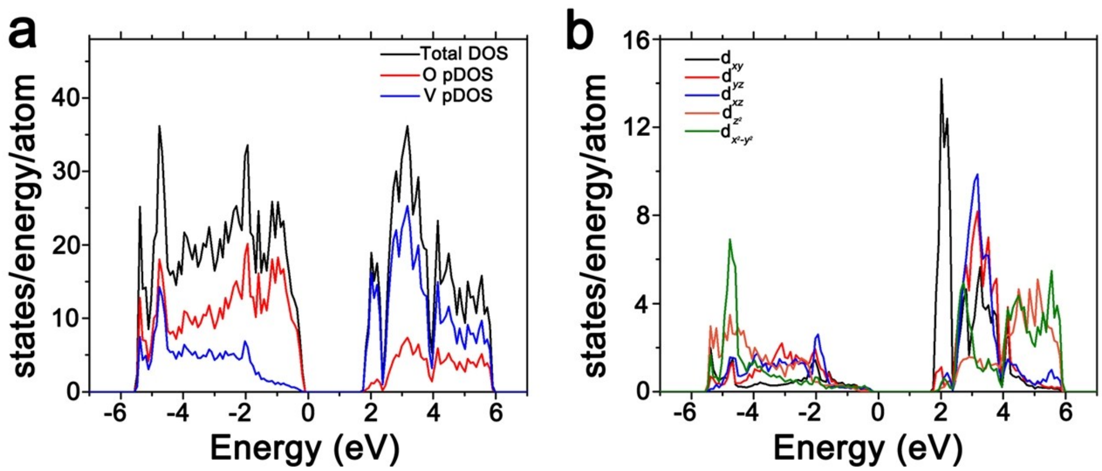

Figure S5. Atom and orbital-projected density of states of V_2O_5. a) atom-projected density of states of V_2O_5 as calculated from density functional theory. The top of the valence band has predominantly O 2p character, whereas the bottom of the conduction band has predominantly V 3d character. **b**) Orbital-projected density of states indicating the splitting of the t_{2g} ($3d_{xy}$, $3d_{xz}$, and $3d_{yz}$) and e_g ($3d_{z2}$, $3d_{x2-y2}$) states as also indicated in Figure 1e.

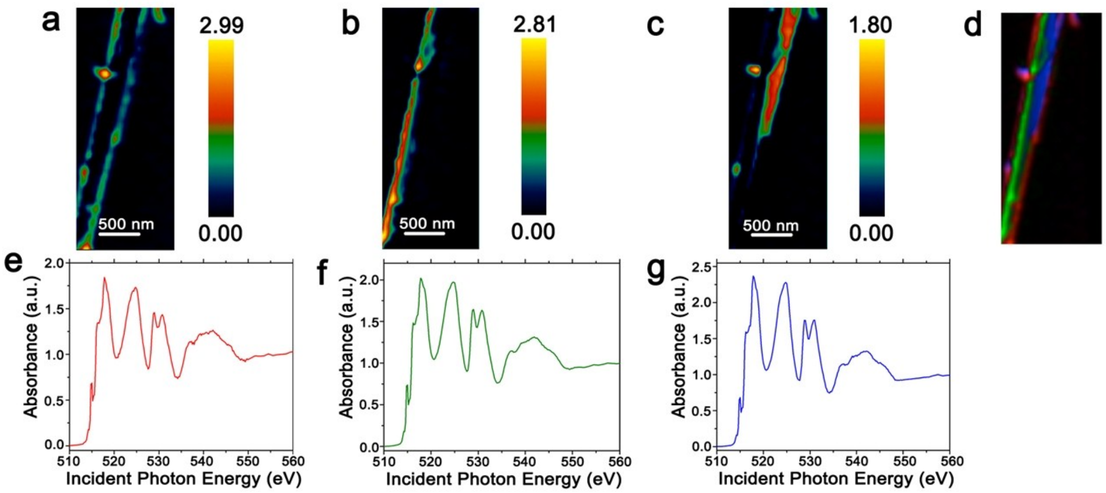

Figure S6. Evaluating electronic structure inhomogeneities and phase separation in V_2O_5 nanowires with extended interfaces. STXM mapping of lithiation profiles across a bundle of closely interfaced nanowires. (a)–(c) depict maps of three spectral components identified by singular value decomposition analysis that are plotted in (e)–(g). While three spectral profiles can be resolved, they are closely related and correspond to the high Li-content δ-phase of $Li_xV_2O_5$. (d) An overlay of the three spectral components illustrating slight variations along the length of the nanowires.

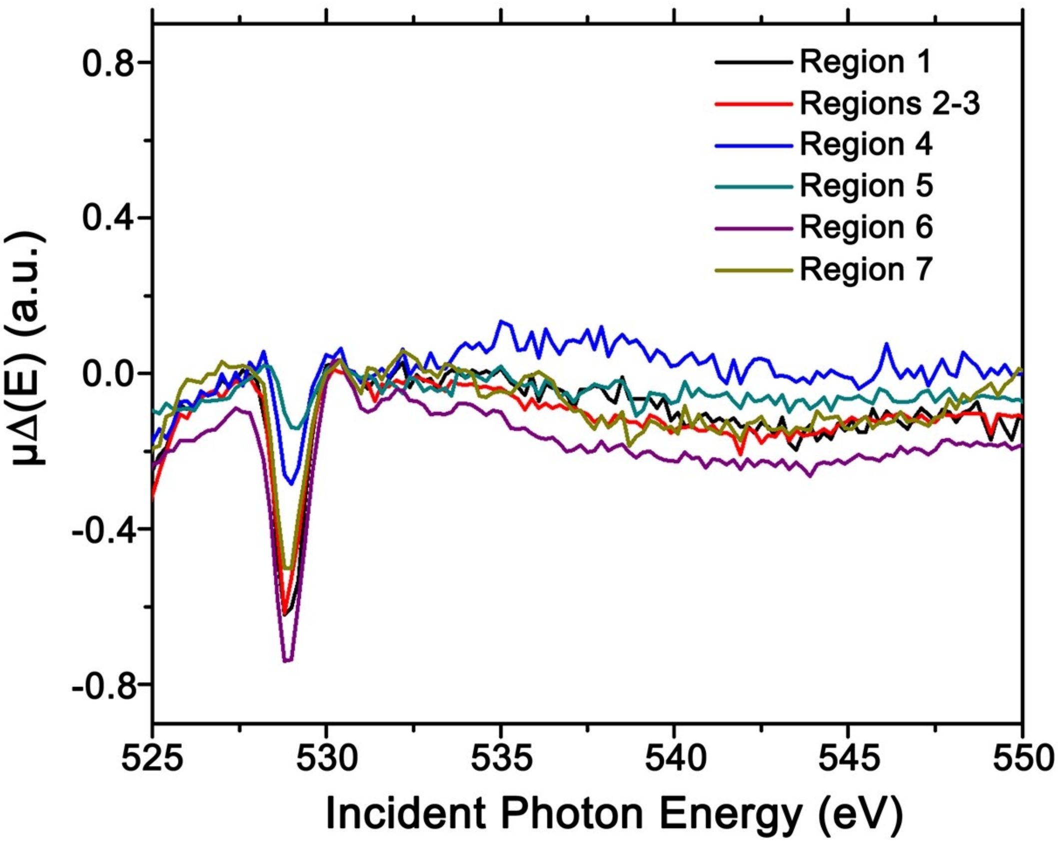

Figure S7. Differential XANES Analysis of Spectral Data. The spectrum for an unlithiated sample was subtracted to the spectrum found for each region of the cluster of wires in Figure 1. All the spectra have been normalized to the e_g absorption feature. The relative intensities allow for assignment of approximate Li-ion concentration.

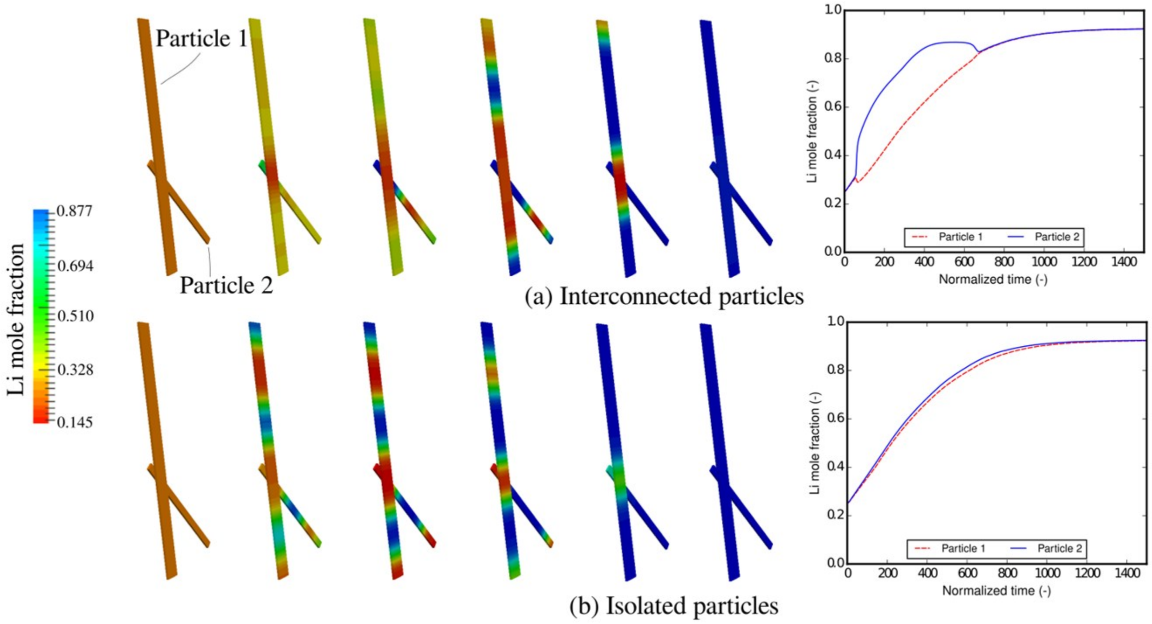

Figure S8. Lithiation in the networks of two particles interconnected to each other (a) and isolated from one other (b). The particles are immersed in a lithium bath with constant potential and lithiated from a homogeneous lithium fraction of 0.25. The contour plots show the snapshots as a function of elapsed time. The curves show the evolution of lithium fraction in each particle: dashed line represents the larger particle, whereas the solid line represents the smaller particle. It is clear that during lithiation, isolated particles experience intraparticular phase separation and are fully lithiated almost at the same time, whereas in interconnected networks with interparticle diffusion allowed it is clear that the smaller particle gets lithiated faster than the connected particle.

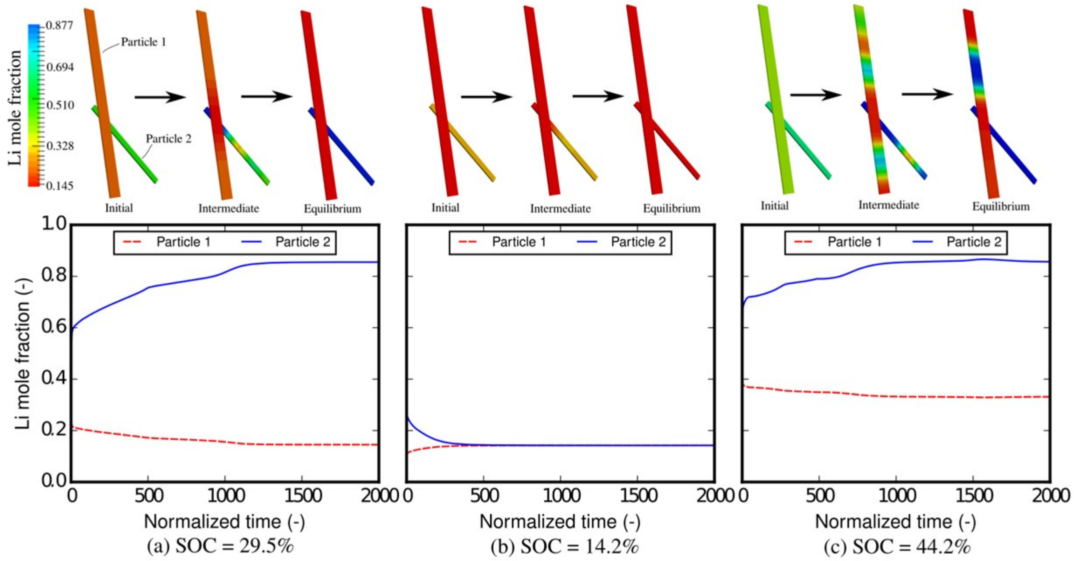

Figure S9. Relaxation of interconnected two particles from non-equilibrium solid-solution with different overall State of Charge (SOC). Contour plots in the upper row show the sequence of relaxation with three different given initial SOC. Curves in the lower row show the respective lithium concentrations in each particle. The blue solid curve represents the smaller particle, whereas the dashed red curve represents the larger particle. The interparticular phase separation occurs when the overall lithium concentration stays in the spinodal region, as shown in (a). On the other hand, when the overall lithium concentration is too low, the complete network will merge into a homogeneous phase, as shown in (b). With increased overall concentration, as shown in (c), phase separation also appears inside a single particle at equilibrium.